Conversion of CH_4 to CH_3OH: Reactions of CoO^+ with CH_4 and D_2, Co^+ with CH_3OD and D_2O, and $Co^+(CH_3OD)$ with Xe

Yu-Min Chen, D. E. Clemmer,† and P. B. Armentrout*

Contribution from the Department of Chemistry, University of Utah, Salt Lake City, Utah 84112

Received January 18, 1994. Revised Manuscript Received April 25, 1994®

Abstract: The mechanisms and energetics involved in the conversion of CH_4 to CH_3OH by CoO^+ are examined by using guided ion beam mass spectrometry. The forward and reverse reactions, $CoO^+ + CH_4 \leftrightarrow Co^+ + CH_3OH$, the collisional activation of $Co^+(CH_3OH)$, and the related reactions, $CoO^+ + D_2 \leftrightarrow Co^+ + D_2O$, are studied. It is found that the oxidations of methane and D_2 by CoO^+, both exothermic reactions, do not occur until overcoming activation barriers of 0.56 ± 0.08 and 0.75 ± 0.04 eV, respectively. The behavior of the forward and reverse reactions in both systems is consistent with reactions that proceed via the insertion intermediates R–Co^+–OH, where R = CH_3 or H. The barrier is probably attributable to a four-centered transition state associated with addition of RH across the CoO^+ bond. In the $Co^+ + CH_3OH$ system (where CH_3OD labeled reactant is used), reactions explained by initial C–H and O–H activation are also observed. The reaction mechanisms and potential energy surfaces for these systems are derived and discussed. Phase space theory calculations are used to help verify these details for the $CoO^+ + D_2$ system. Thermochemistry for several species including $CoOH^+$, CoD^+, CoH, $CoCH_3^+$, $Co^+(CH_3OD)$, $CoOCH_3^+$, and possibly $OCoCH_3^+$ is derived from measurements of reaction thresholds.

Introduction

The direct conversion of methane to methanol has been studied for more than a half century because of its great economic and scientific importance.[1] Although this oxidation reaction,

$$CH_4 + {}^1/_2O_2 \rightarrow CH_3OH \quad \Delta H_{298} = -1.32 \text{ eV} \quad (1)$$

is thermodynamically favored,[2] the best catalyst at present provides a yield of only about 8%.[3] Catalytic conversion of CH_4 to CH_3OH has become an active research area with the search for a more efficient catalyst listed as one of ten challenges for catalysis.[4]

One means of providing fundamental information regarding this process is to study a prototypical gas-phase reaction

$$MO^+ + CH_4 \rightarrow CH_3OH + M^+ \quad (2)$$

Such studies can potentially provide quantitative information regarding the thermodynamics and mechanisms for this process, while simultaneously examining the periodic trends in the chemistry. At present, only a few gas-phase studies of reaction 2 have been made.[5,6] Schröder and Schwarz reported a Fourier transform ion cyclotron resonance (FTICR) study of the reaction of FeO^+ with CH_4.[5] At thermal energies, the reaction produces 57% of $FeOH^+ + CH_3$, 2% of $FeCH_2^+ + H_2O$, and 41% of $Fe^+ + CH_3OH$, which were explained by a reaction mechanism involving a CH_3–Fe^+–OH intermediate. Additional experimental and theoretical studies of various possible intermediates were later conducted as well.[6]

In a recent paper on the reactions of ScO^+, TiO^+, and VO^+ with D_2,[7] we suggested that there should be two main criteria in evaluating the efficiency of reaction 2. First, reaction 2 should be exothermic or thermoneutral. Because the reaction, $O + CH_4 \rightarrow CH_3OH$, has an exothermicity of −3.846 ± 0.005 eV, Table 1, reaction 2 will be *endothermic* for any MO^+ with a bond stronger than 3.85 eV, such as ScO^+, TiO^+, or VO^+, but no other first-row transition-metal ion oxide.[8,9] Second, MO^+ should have a suitable electron configuration such that reaction 2 conserves spin. As discussed elsewhere,[7] CoO^+ is a promising candidate for efficient conversion of CH_4 to CH_3OH. The 0 K bond energy of Co^+–O is 3.25 ± 0.05 eV,[9,10] so reaction 3 is thermodynamically favored.

$$CoO^+ + CH_4 \rightarrow Co^+ + CH_3OH \quad \Delta H_0 = -0.60 \pm 0.05 \text{ eV} \quad (3)$$

Further, it was suggested that CoO^+ has a suitable electron configuration to activate CH_4, and that reaction 3 is spin allowed.[7]

In this paper, we examine the energetics and mechanism of reaction 3 in both the forward and reverse directions, as well as probing how one of its intermediates, $Co^+(CH_3OH)$, decomposes when activated by collisions with Xe. We also study the related but simpler interaction of CoO^+ with D_2 and its reverse, a reaction that has been briefly studied at thermal energies by Schröder et al.[11] We are able to determine a fairly detailed picture of the potential energy surfaces of these reactions and find in both systems that a reaction barrier restricts the oxidation process and its reverse. These conclusions lead to a more careful assessment

† Present address: Department of Chemistry, Northwestern University, 2145 Sheridan, Evanston, IL 60208.

® Abstract published in *Advance ACS Abstracts*, June 15, 1994.

(1) For a review, see: Gesser, H. D.; Hunter, N. R.; Prakash, C. B. *Chem. Rev.* **1988**, *85*, 235.

(2) Lias, S. G.; Bartmess, J. E.; Liebman, J. F.; Holmes, J. L.; Levin, R. D.; Mallard, W. G. *J. Phys. Chem. Ref. Data* **1988**, *17*, Supp. 1 (GIANT tables).

(3) *Chem. Eng. News* **1993**, *May 10*, 22.

(4) *Chem. Eng. News* **1993**, *May 31*, 27.

(5) Schröder, D.; Schwarz, H. *Angew. Chem., Int. Ed. Engl.* **1990**, *29*, 1433. Schwarz, H. *Angew. Chem., Int. Ed. Engl.* **1991**, *30*, 820.

(6) Schröder, D.; Fiedler, A.; Hrušák, J.; Schwarz, H. *J. Am. Chem. Soc.* **1992**, *114*, 1215.

(7) Clemmer, D. E.; Aristov, N.; Armentrout, P. B. *J. Phys. Chem.* **1993**, *97*, 544.

(8) Armentrout, P. B.; Clemmer, D. E. In *Energetics of Organometallic Species*, Simões, J. A. M., Ed.; Kluwer: Netherlands, 1992; p 321.

(9) Armentrout, P. B.; Kickel, B. L. In *Organometallic Ion Chemistry*; Freiser, B. S., Ed.; in press.

(10) Fisher, E. R.; Elkind, J. L.; Clemmer, D. E.; Georgiadis, R.; Loh. S. K.; Aristov, N.; Sunderlin, L. S.; Armentrout, P. B. *J. Chem. Phys.* **1990**, *93*, 2676. The value cited here is an average value reassessed in ref 9.

(11) Schröder, D.; Fiedler, A.; Ryan, R. F.; Schwarz, H. *J. Phys. Chem.* **1994**, *98*, 68.

0002-7863/94/1516-7815$04.50/0

Table 1. Bond Energies and Enthalpies of Formation at 0 K

species	$\Delta_f H_0$ (eV)	bond	D_0 (eV)
O	2.558(0.001)[a]	Co^+–O	3.25(0.05)[b]
H	2.239[a]	Co^+–H	1.98(0.06)[c]
D	2.278[a]	Co^+–D	2.01(0.06),[c] 2.05(0.05)[d]
OH	0.405(0.003)[e]	Co–H	1.86(0.05),[f] 1.89(0.06)[d]
OD	0.382(0.001)[e]	Co^+–OH	3.13(0.04),[d] 3.12(0.13),[g] 3.08(0.13)[h]
CH_2	4.02(0.03)[i]	Co^+–CH_2	3.29(0.05)[j]
CH_3	1.553(0.004)[k]	Co^+–CH_3	2.10(0.04),[l] 2.10(0.08)[d]
H_2O	−2.476(0.001)[a]	Co^+–H_2O	1.67(0.06),[m] 1.61(0.13),[g] 1.74(0.2)[n]
HDO	−2.513(0.001)[a]		
D_2O	−2.552(0.001)[a]		
CH_2O	−1.086(0.005)[o,p]		
CH_2OH	−0.12(0.01)[q]		
CH_3O	0.25(0.04)[k]	Co^+–OCH_3	≥3.0(0.3),[d] ≥1.8[r]
CH_3OH	−1.976(0.003)[o,s]	OCo^+–CH_3	≥2.32(0.05)[d]
CH_3OD	−2.005(0.003)[t]	Co^+–CH_3OD	1.53(0.08)[d]
CH_4	−0.688(0.004)[o,p]		

[a] Chase, M. W.; Davies, C. A.; Downey, J. R.; Frurip, D. J.; McDonald, R. A.; Syverud, A. N. *J. Phys. Chem. Ref. Data* **1985**, *14*, Suppl. No. 1 (JANAF Tables). [b] References 10 and 9. [c] Reference 36. [d] This work. [e] Gurvich, L. V.; Veyts, I. V.; Alcock, C. B. *Thermodynamic Properties of Individual Substances*, 4th ed.; Hemisphere: New York, 1989; Vol. 1, Part 2. [f] Reference 38. [g] Reference 28. No temperature specified. [h] Reference 29. No temperature specified. [i] Leopold, D. G.; Murray, K. K.; Stevens Miller, A. E.; Lineberger, W. C. *J. Chem. Phys.* **1985**, *83*, 4849. [j] Reference 16. [k] Berkowitz, J.; Ellison, G. B.; Gutman, D. *J. Phys. Chem.*, in press. [l] Reference 35. [m] Reference 39. [n] 298 K value from ref 44. [o] $\Delta_f H_{298}$ value of: Pedley, J. B. Naylor, R. D.; Kirby, S. P. *Thermochemical Data of Organic Compounds*, 2nd ed.; Chapman and Hall: New York, 1986. [p] Adjusted to 0 K by using information in footnote *a*. [q] Average of values in ref 37 and footnote *k*. [r] Derived from results in ref 33. [s] Adjusted to 0 K by using information in footnote *t*. [t] Value taken from the following and adjusted for $\Delta_f H(CH_3OH)$ used here: Chen, S. S.; Wilhoit, R. C.; Zwolinski, B. J. *J. Phys. Chem. Ref. Data* **1977**, *6*, 105.

of the ground-state electron configuration for CoO^+ and its suitability for activation of CH_4.

Experimental Section

General Procedures. The guided ion beam instrument on which these experiments were performed has been described in detail previously.[12,13] Ions are created in a flow tube source, described below. The ions are extracted from the source, accelerated, and focused into a magnetic sector momentum analyzer for mass analysis. Mass-selected ions are slowed to a desired kinetic energy and focused into an rf octopole ion guide that radially traps the ions.[14] The octopole passes through a static gas cell containing the neutral reactant. Gas pressures in the cell are kept low (between 0.08 and 0.3 mTorr) so that multiple ion–molecule collisions are improbable. All results reported here are due to single bimolecular encounters, as verified by pressure dependent studies. Product and unreacted beam ions are contained in the guide until they drift out of the gas cell where they are focused into a quadrupole mass filter for mass analysis and then detected. Ion intensities are converted to absolute cross sections as described previously.[12] Uncertainties in cross sections are estimated to be ±20%.

Laboratory ion energies (lab) are converted to energies in the center-of-mass frame (CM) by using the formula $E_{CM} = E_{lab}m/(m+M)$, where M and m are the ion and neutral reactant masses, respectively. The absolute zero and distribution of the ion kinetic energy are determined by using the octopole beam guide as a retarding potential analyzer.[12] The uncertainty in the absolute energy scale is ±0.05 eV (lab). The distribution of ion energies is nearly Gaussian and has an average fwhm of about 0.35 eV (lab). Unless otherwise stated, all energies cited below are in the CM frame.

CH_3OD, D_2, and D_2O are obtained from Cambridge Isotope Laboratories with purity stated as 99%, 99.8%, and 99.9%, respectively, and CH_4 is obtained from Matheson with a purity stated as 99.99%. CH_4 and D_2 were used directly without further purification, and CH_3OD and D_2O were purified by several freeze–pump–thaw cycles with liquid N_2 to eliminate noncondensible impurities before use.

Ion Source. Cobalt ions are produced in a dc-discharge flow tube (DC/FT) source.[13,15] The flow gases used in this experiment are He and Ar, maintained at pressures of ~0.65 and ~0.06 Torr, respectively. A dc discharge at a voltage of ~2.2 kV is used to ionize argon and then accelerate these ions into a cobalt metal cathode to create Co^+ ions. The ions are then swept down a meter-long flow tube by the He and Ar flow gases and undergo ~10^5 collisions with the flow gases. Trace amounts of high-lying excited states (>2.1 eV) can survive these flow conditions, but they are easily removed by introducing O_2 to the flow tube several centimeters downstream at a pressure of ~2 mTorr. We believe these conditions produce Co^+ ions in their ground electronic state. All results reported here are consistent with this, as are tests involving a number of other reactions.[16]

CoO^+ was produced in the flow tube by introducing N_2O at a pressure of less than 1 mTorr, together with He and Ar flowing through the dc-discharge source. The reaction of Co^+ with N_2O to form CoO^+ is exothermic by about 1.6 eV, but it is observed to be inefficient at low collision energies.[17] $Co^+(CH_3OD)$ was produced in the flow tube by three-body stabilization of Co^+ with CH_3OD, introduced at a pressure of less than 1 mTorr at the midpoint of the flow tube. The CoO^+ and $Co^+(CH_3OD)$ ions are cooled by ~10^5 collisions with the flow gases. Collision-induced dissociation (CID) of CoO^+ with Xe is consistent with ions that are not internally excited. We assume that these ions are in their ground electronic states and that the internal energy of these clusters is well described by a Maxwell–Boltzmann distribution of rotational and vibrational states corresponding to 298 K. Previous work from this laboratory[15,18-23] has shown that these assumptions are valid.

Data Analysis. Cross sections are modeled by using eq 4,[24]

$$\sigma(E) = \sigma_o \sum_i g_i (E + E_i + E_{rot} - E_0)^n / E \qquad (4)$$

where E is the relative kinetic energy of the ions, E_0 is the 0 K reaction threshold, σ_o is an energy-independent scaling factor, and n is an adjustable parameter. Equation 4 takes into account the thermal internal energy of the reactants by treating the calculated cross section as a sum over vibrational states (with energies E_i and populations g_i) as described previously,[15] and by including the thermal rotational energy. In this study, the vibrational energies of D_2, CH_4, and CoO^+ at 298 K are negligible; only the vibrational energies of CH_3OD and $Co^+(CH_3OD)$ were included in eq 4. The vibrational frequencies of CH_3OD were taken from Shimanouchi.[25] No vibrational frequencies are available for $Co^+(CH_3OD)$, so we estimated these frequencies as the vibrational frequencies of CH_3OD plus three cobalt–methanol vibrational frequencies (one stretching and two bending) of 330, 192, and 106 cm^{-1}.[26] The total rotational energy of the reactants at 298 K is $E_{rot} = 3k_BT/2 = 0.039$ eV for the $Co^+ + D_2O$, $Co^+ + CH_3OD$, and $Co^+(CH_3OH) + Xe$ systems, $2k_BT = 0.053$ eV for the $CoO^+ + D_2$ system, and $5k_BT/2 = 0.066$ eV for the $CoO^+ + CH_4$ system. Before comparison with the data, eq 4 must be convoluted over the reactant neutral and ion kinetic energy distributions, as described previously.[12]

(12) Ervin, K. M.; Armentrout, P. B. *J. Chem. Phys.* **1985**, *83*, 166.
(13) Schultz, R. H.; Armentrout, P. B. *Int. J. Mass Spectrom. Ion Processes* **1991**, *107*, 29.
(14) Teloy, E.; Gerlich, D. *Chem. Phys.* **1974**, *4*, 417. Gerlich, D. Diplomarbeit, University of Freiburg, Federal Republic of Germany, 1971.
(15) Schultz, R. H.; Crellin, K. C.; Armentrout, P. B. *J. Am. Chem. Soc.* **1991**, *113*, 8590.
(16) Haynes, C. L.; Armentrout, P. B. *Organometallics*, accepted for publication.
(17) Armentrout, P. B.; Halle, L. F.; Beauchamp, J. L. *J. Chem. Phys.* **1982**, *76*, 2449.
(18) Schultz, R. H.; Armentrout, P. B. *J. Chem. Phys.* **1992**, *96*, 1046.
(19) Khan, F. A.; Clemmer, D. C.; Schultz, R. H.; Armentrout, P. B. *J. Phys. Chem.* **1993**, *97*, 7978.
(20) Fisher, E. R.; Kickel, B. L.; Armentrout, P. B. *J. Phys. Chem.* **1993**, *97*, 10204.
(21) Fisher, E. R.; Kickel, B. L.; Armentrout, P. B. *J. Chem. Phys.* **1992**, *97*, 4859.
(22) Dalleska, N. F.; Honma, K.; Armentrout, P. B. *J. Am. Chem. Soc.* **1993**, *115*, 12125.
(23) Chen, Y.-M.; Armentrout, P. B. *Chem. Phys. Lett.* **1993**, *210*, 123.
(24) Armentrout, P. B. In *Advances in Gas Phase Ion Chemistry*; Adams, N. G.; Babcock, L. M., Eds.; JAI: Greenwich, 1992; Vol. 1, p 83.
(25) Shimanouchi, T. *Tables of Molecular Vibrational Frequencies Consolidated*; NSRDS-NBS No. 39, 1972; Vol. 1.
(26) These three frequencies were estimated from a theoretical calculation for $Mg^+(CH_3OH)$: Sodupe, M.; Bauschlicher, C. W. *Chem. Phys. Lett.* **1992**, 195, 494. The stretching mode at 415 cm^{-1} was scaled to 330 cm^{-1} by using a Morse potential model, and the two bending mode frequencies were used without modification. Variation of these frequencies by ±30% has no significant effect on the threshold analysis.

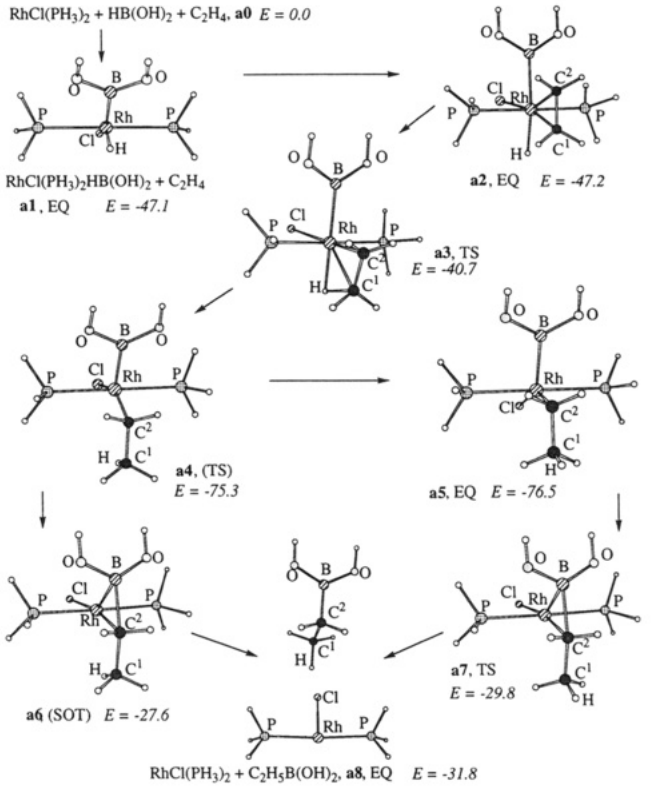

Figure 1. The critical structures of the **I.1.A** mechanism of the reaction $HB(OH)_2 + C_2H_4 + ClRh(PH_3)_2 \rightarrow ClRh(PH_3)_2 + C_2H_5B(OH)_2$. EQ, TS, and SOT stand for equilibrium, transition state, and second order top geometries, with parentheses indicating that one of the estimated imaginary frequencies is not related to the reaction.

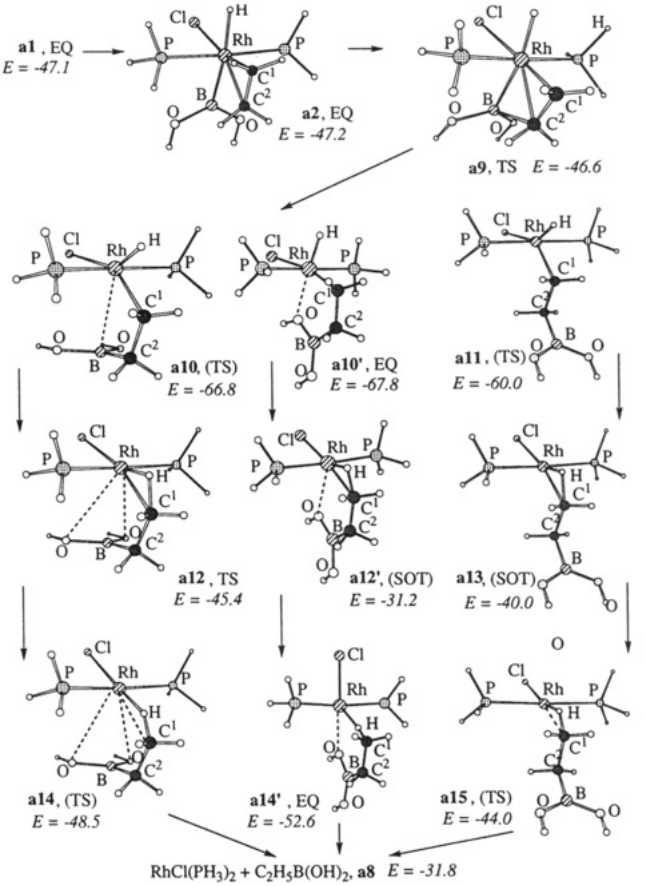

Figure 2. The critical structures of the **I.1.B** mechanism of the reaction $HB(OH)_2 + C_2H_4 + ClRh(PH_3)_2 \rightarrow ClRh(PH_3)_2 + C_2H_5B(OH)_2$. See Figure 1 for notation.

calculated and observed ∠PRhCl angles differ only by about 1°. Our ∠ClRhB angle is 10° larger than the experiment; we do not know at the moment the reason for this discrepancy.

The exothermicity of the oxidative addition of $HB(OH)_2$ to $RhCl(PH_3)_2$ is calculated to be 47.1 kcal/mol at the MP2/I// MP2/I level. However, this number might be overestimated by several kcal/mol because of basis set superposition error.[15-17]

Mechanism I.1.A. Coordination of ethylene to $Rh(H)Cl(PH_3)_2[B(OH)_2]$ (**a1**) between H and $B(OH)_2$ ligands gives the complex $Rh(H)Cl(PH_3)_2[B(OH)_2](C_2H_4)$ (**a2**). The rhodium atom in **a2** is six-coordinated and has nearly an octahedral environment. The ∠ClRhB and ∠ClRhH angles are reduced to 80.8° and 85.4°, respectively, and ∠BRhX and ∠HRhX angles, where X is the center of the C=C bond, are in the range of 90−100°. The Rh−H and Rh−B bond lengths are elongated by about 0.1 Å, relative to **a1**. The C−C bond is 1.467 Å, stretched by 0.12 Å as compared to the free C_2H_4 molecule and close to those in metallocycle structures.[18] The Rh−C^1 and Rh−C^2 distances are 2.124 and 2.161 Å, respectively, which also are close to those for Rh−C covalent bond.[18] Thus, **a2** has a metallocycle structure.

The binding energy $Rh(H)Cl(PH_3)_2[B(OH)_2](C_2H_4)$ (**a2**) → $Rh(H)Cl(PH_3)_2[B(OH)_2] + C_2H_4$ is calculated to be only 0.1 kcal/mol, a surprising small value. The reason of this is that the attack of the C_2H_4 to **a1** between H and $B(OH)_2$ ligands is highly unfavorable. In order to find the origin of the small binding energy, we divide this binding energy ΔE into three parts:

$$\Delta E = \mathrm{DEF}(\mathbf{a1}) + \mathrm{DEF}(C_2H_4) + \mathrm{INT} \qquad (2)$$

DEFs are energies required to deform the reactant fragments, **a1** and C_2H_4, from their respective equilibrium geometries to the geometries in the product complex **a2**. INT is the interaction energy between the deformed fragments. Table 3 shows that the energy required to open the narrowest angle of Y to make it a T shape is extremely large (66 kcal/mol), compared to those required to open the wider angle fo Y to make a T to be discussed later with the product **a16** and **a19**. Since the product **a2** is a metallocycle, the interaction energy INT is large in magnitude but cannot compensate the large DEF.

The reaction proceeds further via migratory insertion of the C=C bond into the Rh−H bond through TS (**a3**), which is an early transition state, in accord with high exothermicity of the **a2** → **a3** → **a4** process. Table 2 shows that the Rh−H bond in **a3** is only 0.045 Å longer than in **a2**, and the C−C distance has not changed. Although the C^1−H distance in **a3** is 0.7 Å shorter than in **a2**, it is still very far from the regular C−H bond length. The Rh−C^1 distance is lengthened by about 0.1 to 2.22 Å in **a3**, but the bond is still preserved in the TS. Geometry of the reacting fragment has a double three-centered character, with H, C^1, and C^2 all interacting with Rh. The barrier height is 6.5 kcal/mol relative to **a2**, and **a3** lies substantially below the initial reactants, $RhCl(PH_3)_2 + HB(OH)_2 + C_2H_4$ (**a0**).

Insertion maintaining C_s symmetry results in the complex **a4**, $RhCl(PH_3)_2[B(OH)_2](C_2H_5)$, which is 28.2 kcal/mol lower than

(15) (a) Morokuma, K.; Kitaura, K. *In Chemical Application of Atomic and Molecular Electrostatic Potentials*; Politzer, P., Truhler, D. G., Eds.; Plenium: New York, 1981. (b) Kitaura, K.; Sakaki, S.; Morokuma, K. *Inorg. Chem.* **1981**, *20*, 2292.

(16) Frish, M. J.; Del Bene, J. E.; Binkley, J. S.; Schaefer, III, H. F. *J. Chem. Phys.* **1986**, *84*, 2279.

(17) Koga, N.; Morokuma, K. *J. Am. Chem. Soc.* **1993**, *115*, 6883.

(18) Sodupe, M.; Bauschlicher Jr., C. W.; Langhoff, S. R.; Partridge, H. *J. Phys. Chem.* **1992**, *96*, 2118.

Table 2. Summary of Fitting Parameters of Eq 4 Used to Model Reaction Cross Sections[a]

reactions		σ_0	n	E_0
$Co^+ + D_2O$	$\rightarrow CoD^+ + OD$	0.86(0.08)	1.2(0.1)	3.16(0.05)
	$\rightarrow CoOD^+ + D$	0.11(0.03)	1.8(0.3)	2.11(0.12)
$CoO^+ + D_2$	$\rightarrow CoOD^+ + D$	1.62(0.13)	2.1(0.2)	0.75(0.04)
	$\rightarrow CO^+ + D_2O$	0.20(0.05)	1.9(0.2)	0.60(0.15)
	$\rightarrow CO^+ + [O + D_2]$	1.96(0.15)	0.9(0.1)	3.32(0.09)
	$\rightarrow CoD^+ + OD$	0.12(0.04)	1.9(0.2)	1.46(0.13)
$Co^+ + CH_3OD$	$\rightarrow CoOD^+ + CH_3$	2.99(0.12)	1.1(0.2)	0.81(0.04)
	$\rightarrow CoCH_3^+ + OD$	1.10(0.19)	1.9(0.2)	1.84(0.08)
	$\rightarrow CH_2OD^+ + CoH$	1.06(0.12)	1.4(0.2)	1.89(0.06)
	$\rightarrow CoH^+ + CH_2OD$	0.73(0.10)	1.7(0.1)	$\equiv$2.12
	$\rightarrow CoD^+ + CH_3O$	0.19(0.04)	1.5(0.2)	2.80(0.12)
	$\rightarrow CoOCH_3^+ + D$			$\sim$1.5(0.3)
	$\rightarrow CoCH_2^+ + DOH$	0.06(0.02)	2.0(0.2)	0.90(0.08)
$CoO^+ + CH_4$	$\rightarrow CoOH^+ + CH_3$	0.46(0.05)	1.7(0.1)	0.56(0.08)
	$\rightarrow Co^+ + CH_3OH$	0.05(0.02)	2.6(0.2)	0.56(0.08)
	$\rightarrow Co^+ + [O + CH_4]$	0.53(0.16)	1.4(0.2)	3.29(0.07)
	$\rightarrow CoH^+ + CH_2O + H$	0.20(0.05)	1.7(0.2)	2.66(0.12)
	$\rightarrow CoOCH_3^+ + H$	0.23(0.03)	1.3(0.1)	2.15(0.05)
$Co^+(CH_3OD) + Xe$	$\rightarrow Co^+ + CH_3OD^+ Xe$	2.55(0.32)	1.5(0.1)	1.53(0.08)

[a] Uncertainties of one standard deviation are in parentheses.

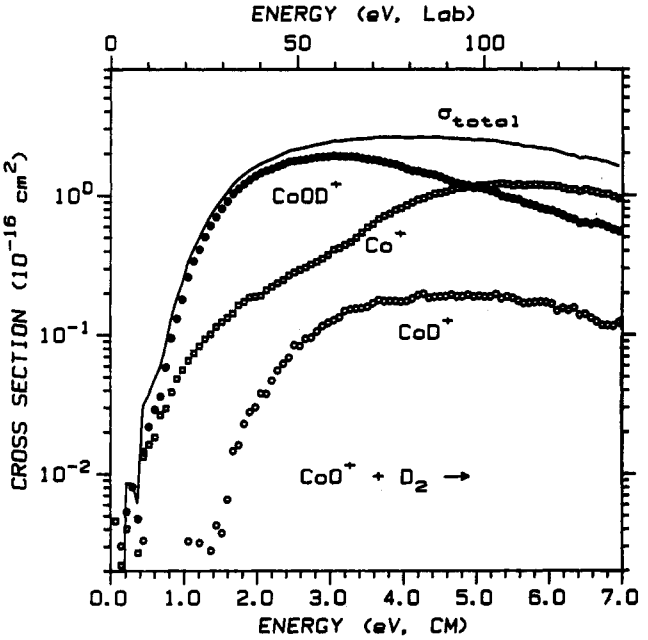

Figure 2. Cross sections for reactions of CoO^+ with D_2 as a function of kinetic energy in the center-of-mass frame (lower axis) and laboratory frame (upper axis).

with two contributions to eq 4 as given in Table 2. The high energy part begins at an energy consistent with either reaction 8b or 8c. Analysis of the cross section below 3 eV yields E_0 = 0.60 ± 0.15 eV, within experimental error of the threshold measured for reaction 7, 0.75 ± 0.04 eV. It was verified that both of these threshold measurements did not depend on the pressure of the D_2 reactant within the cited experimental error.

Our results for this system differ from those of Schröder et al.,[11] who found that only reaction 8a was observed with a thermal rate constant of 1.2×10^{-12} cm^3/s. Below 0.4 eV, our cross sections for this reaction and for reaction 7 have reached the noise level and are both about $(3 \pm 5) \times 10^{-3}$ Å^2, respectively. If our data are converted to rate constants, the values are about $0.9 \pm 1.5 \times 10^{-13}$ cm^3/s for both reactions. Both the cross sections and rate constants are probably best viewed as upper limits. The reasons behind the discrepancy between our rate constant and that of Schröder et al. are unclear.[32]

$Co^+ + CH_3OD$. Translationally excited cobalt ions react with methanol deuterated at the hydroxy position to yield seven ionic products, formed in reactions 10–16.

$$CO^+ + CH_3OD \rightarrow CoOD^+ + CH_3 - 0.84 \pm 0.09 \text{ eV} \quad (10)$$

$$\rightarrow CoCH_3^+ + OD - 1.84 \pm 0.04 \text{ eV} \quad (11)$$

$$\rightarrow CH_2OD^+ + CoH - 1.92 \pm 0.05 \text{ eV} \quad (12)$$

$$\rightarrow CoH^+ + CH_3OD - 2.12 \pm 0.06 \text{ eV} \quad (13)$$

$$\rightarrow CoD^+ + CH_3O - 2.52 \pm 0.07 \text{ eV} \quad (14)$$

$$\rightarrow CoOCH_3^+ + D \quad (15)$$

$$\rightarrow CoCH_2^+ + HOD - 0.22 \pm 0.06 \text{ eV} \quad (16)$$

These results are shown in Figure 3. Reactions 10 and 11, which correspond to activation of the C–O bond, dominate the product spectrum at low energies. Competition between the $CoOD^+$ and $CoCH_3^+$ products is suggested by the observation that the former cross section reaches a peak at the threshold for the latter. These products both decline rapidly above ~4 eV, which corresponds to $D_0(CH_3\text{–}OD)$ = 3.940 ± 0.005 eV, indicating that they decompose to $Co^+ + CH_3 + OD$. Activation of the C–H bond leads to reactions 12 and 13, where the products differ only in the location of the charge. These reactions are the most likely processes at high energies, in part because of angular momentum considerations. Activation of the single O–D bond is energetically and statistically less favorable than activation of the three available C–H bonds. This is reflected in the small size of the CoD^+ and $CoOCH_3^+$ products. Note that the $CoOCH_3^+$ cross section peaks at the threshold for CoD^+ formation, indicating competition between these products. Also, the complex rearrangement of the reactants to eliminate water, reaction 16, is relatively unlikely.

Analyses of these various cross sections yield the optimum parameters given in Table 2. The thresholds for reactions 10–12 are in good agreement with those calculated from literature thermochemistry. The cross section for CoH^+ is somewhat scattered because this product has a mass close to that of the

(32) There are a couple of explanations for the discrepancy that may be worth considering. One is that we do not observe this reaction because of kinetic shift problems. This is discussed in detail below, where we conclude that this explanation is probably not the problem. Another possibility is that Schröder et al. have excited CoO^+ ions, but this would mean that all or most of their ions would have to be excited. This may be plausible because the CoO^+ ions are formed by reaction of $Co^+ + N_2O$, a reaction that may preferentially form excited triplet CoO^+ ions due to spin-conservation.

much more intense reactant. This makes analysis of the data difficult, although this cross section is easily reproduced if the thermodynamic threshold is used in eq 4. Analysis of the cross section for reaction 14 yields an E_0 value that is slightly larger than the thermodynamic value, but well below that for production of $CoD^+ + CH_2O + H$, 3.43 ± 0.06 eV. The measured threshold is probably elevated because of competition with the other much more likely reaction channels. The small size of the $CoOCH_3^+$ cross section makes definitive analysis difficult, although an estimate of the threshold is 1.5 ± 0.3 eV. Analysis of the $CoCH_2^+$ cross section yields E_0 = 0.90 ± 0.08 eV, considerably above the thermodynamic threshold of 0.22 ± 0.06 eV. This may be due to competition with the other more likely channels, but the complexity of this rearrangement means that the possibility of a reaction barrier needs to be considered, as discussed further below.

As in the $Co^+ + D_2O$ system, CoO^+ was not observed in the reaction of Co^+ with CH_3OD even though formation of $CoO^+ + CH_3D$ has the second lowest overall reaction endoergicity, 0.60 ± 0.05 eV (ignoring the effects of deuterium substitution). A careful search for this product indicates that its cross section is less than 0.02 Å^2.

$CoO^+ + CH_4$. Translationally excited cobalt oxide ions react with methane to form five ionic products, corresponding to processes 17–21, as shown in Figure 4.

$$CoO^+ + CH_4 \rightarrow CoOH^+ + CH_3 - 0.24 \pm 0.10 \text{ eV} \quad (17)$$

$$\rightarrow Co^+ + CH_3OH + 0.60 \pm 0.05 \text{ eV} \quad (18a)$$

$$\rightarrow Co^+ + O + CH_4 - 3.25 \pm 0.05 \text{ eV} \quad (18b)$$

$$\rightarrow Co^+ + OH + CH_3 - 3.34 \pm 0.05 \text{ eV} \quad (18c)$$

$$\rightarrow CoH^+ + CH_2O + H - 2.79 \pm 0.08 \text{ eV} \quad (19)$$

$$\rightarrow CoOCH_3^+ + H \quad (20)$$

$$\rightarrow CoOCH_2^+ + 2\,H \quad (21)$$

It can be seen that the cross sections for reactions 17 and 18 behave similarly to those for the analogous reactions 7 and 8 in the $CoO^+ + D_2$ reaction system. Also, the products observed in this system are similar to those seen in the $Co^+ + CH_3OD$ system, with the notable absence of $CoCH_3^+$, CH_3O^+ (corresponding to the CH_2OD^+ product), and $CoCH_2^+$ (even though formation of $CoCH_2^+ + H_2O$ is exothermic by 0.37 ± 0.08 eV). Searches for these three products were conducted and our failure to observe them indicates they have cross sections less than 0.02 Å^2, although efficient detection of the $CoCH_3^+$ product is more problematic because it is only one mass unit away from the much more intense reactant ion.

As in the $CoO^+ + D_2$ system, the exothermic oxidation reaction 18a, does not occur until overcoming an activation barrier of 0.5–1.0 eV, nearly the same energy required to form $CoOH^+$, the dominant product at low energies. It was verified that these reaction cross sections are not dependent on the pressure of the CH_4 reactant within our experimental error. Reactions 18b and 18c account for the increased production of Co^+ observed above ~3 eV. Competition between the Co^+ and $CoOH^+$ channels is suggested by the smooth variation in the total cross section with energy. Analysis of the cross section for $CoOH^+$ with eq 4, Table 2, yields E_0 = 0.56 ± 0.08 eV, about 0.3 eV larger than the thermodynamic threshold of 0.24 ± 0.10 eV. The data cannot be reproduced well if the thermodynamic threshold is used in eq 4. Analysis of the Co^+ cross section is difficult because this cross section rises very slowly and has both low and high energy components. The low energy portion of the data can be reproduced nicely with E_0 = 0.56 ± 0.08 eV, the same as for the $CoOH^+$ channel. The high energy portion of the Co^+ cross section can be reproduced by adding a cross section beginning at 3.29 ± 0.07 eV, consistent with reactions 18b and 18c.

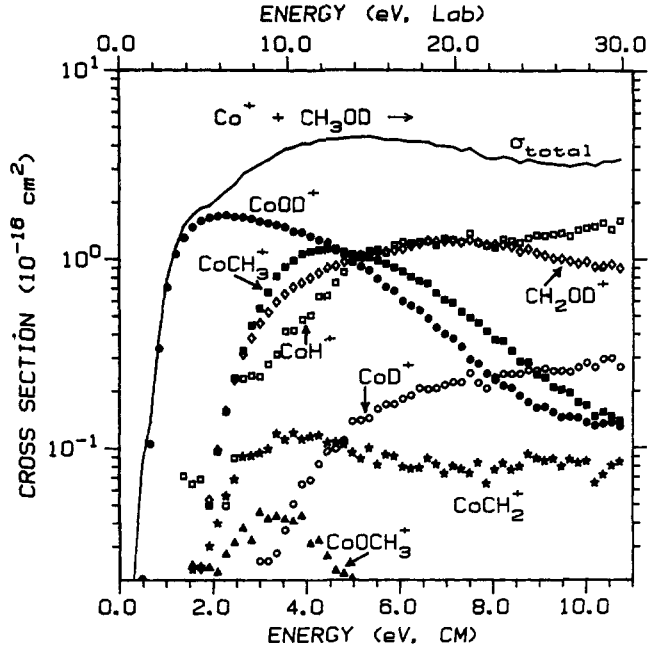

Figure 3. Cross sections for reactions of Co^+ with CH_3OD as a function of kinetic energy in the center-of-mass frame (lower axis) and laboratory frame (upper axis).

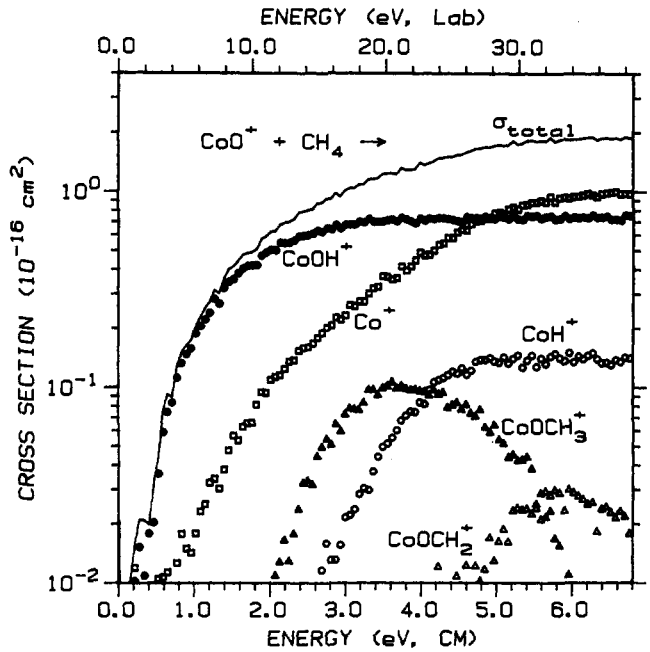

Figure 4. Cross sections for reactions of CoO^+ with CH_4 as a function of kinetic energy in the center-of-mass frame (lower axis) and laboratory frame (upper axis).

Formation of both $CoOCH_3^+ + H$ and $CoOH^+ + CH_3$ involves activation of the C–H bond of methane followed by loss of one of the radicals thus formed. Production of $CoOCH_3^+$ appears to be suppressed because it has a threshold 1.6 eV higher than that for $CoOH^+$, Table 2. Also angular momentum constraints inhibit this channel relative to the $CoOH^+$ channel. Formation of $CoOCH_2^+$ appears to proceed by hydrogen atom loss from the $CoOCH_3^+$ based on its high threshold energy and its energy dependence, but the cross section is too small to analyze definitively. Analysis of the CoH^+ cross section, Table 2, yields

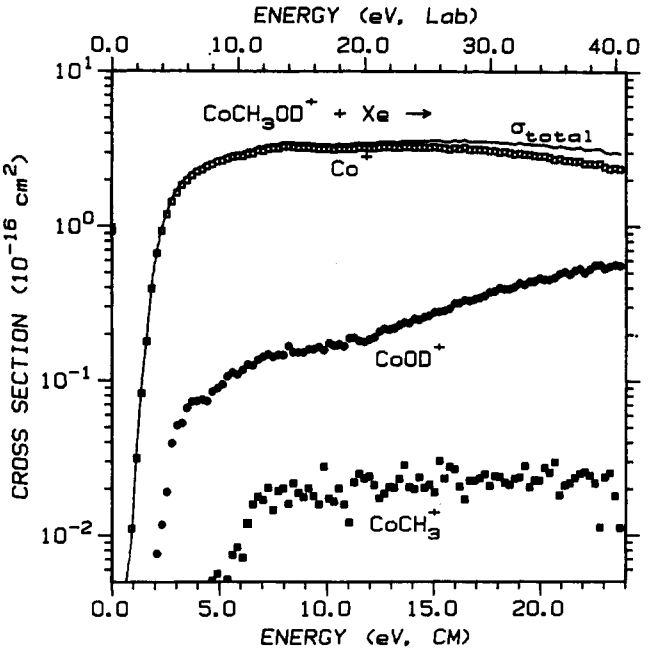

Figure 5. Cross sections for reactions of $Co^+(CH_3OD)$ with Xe as a function of kinetic energy in the center-of-mass frame (lower axis) and laboratory frame (upper axis).

E_0 = 2.66 ± 0.12 eV, considerably above the thermodynamic threshold for formation of $CoH^+ + CH_3O$, 1.89 ± 0.09 eV. Although this could be because of competition with the predominant reaction channels, another possibility is that the observed reaction corresponds to formation of $CoH^+ + CH_2O + H$, which can begin at 2.79 ± 0.08 eV, within experimental error of the measured threshold. This hypothesis is consistent with the observations that the $CoOCH_3^+$ product cross section begins to decline at about this energy and that the sum of these two cross sections is a smooth function of energy. It is also consistent with the observations of Freiser and co-workers on the decomposition of $CoOCH_3^+$ ions.[33]

$Co^+(CH_3OD)$ + Xe. Three ionic products are observed when $Co^+(CH_3OD)$ is activated by collision with Xe, Figure 5. These correspond to processes 22–24.

$$Co^+(CH_3OD) + Xe \rightarrow Co^+ + CH_3OD + Xe \quad (22)$$

$$\rightarrow CoOD^+ + CH_3 + Xe \quad (23)$$

$$\rightarrow CoCH_3^+ + OD + Xe \quad (24)$$

Reaction 22, the collision-induced dissociation (CID) of $Co^+(CH_3OD)$, dominates the product spectrum over the experimental energy region shown in Figure 5, because this reaction is a simple bond cleavage process. Reactions 23 and 24, which correspond to the activation of the C–O bond, are minor, unlike in the reaction system of $Co^+ + CH_3OD$. The products corresponding to the activation of C–H and O–D bonds, such as CH_2OD^+, CoH^+, CoD^+, and $CoOCH_3^+$, were looked for carefully, but not observed. This indicates that their cross sections are less than 0.01 Å^2. This is due to the strong competition from the CID reaction which suppresses all but the major reactions observed in the bimolecular $Co^+ + CH_3OD$ reaction system.

Analysis of the cross section for reaction 22 yields the optimum parameters given in Table 2. Analysis of the $CoOD^+$ cross section is difficult, because this cross section appears to have both a low-energy component and a high-energy component, obvious above about 12 eV. If the calculated, thermodynamic threshold of 2.34 ± 0.09 eV (the sum of the thresholds for reactions 10 and 22) is used in eq 4, the low-energy portion of the cross section can be reproduced. The high-energy portion may be due to a distinct pathway for formation of $CoOD^+$ or to another isomer, D–Co^+–O, which would lie about 2.3 eV higher than $CoOD^+$ assuming that $D_0(OCo^+–D) \approx D_0(Co^+–D)$. Analysis of reaction 24 was not performed because the cross section is small and rises slowly from its onset.

Thermochemical Results. (a) $CoOH^+$. As shown in Figures 1–5, $CoOD^+$ or $CoOH^+$ is observed in all five of the reaction systems studied here. In the following discussion, we assume that the Co^+–OH and Co^+–OD bond energies are identical, a reasonable assumption, as discussed elsewhere.[34] Thresholds measured for reactions 6, 7, 10, and 17 lead to Co^+–OH bond energies of 3.10 ± 0.12, 2.60 ± 0.07, 3.13 ± 0.04, and 2.78 ± 0.10 eV. The two larger values agree with the literature: 3.12 ± 0.13 eV obtained from a CID study by Magnera, David, and Michl,[28] and 3.08 ± 0.13 eV obtained by photodissociation of $CoOH^+$ by Cassady and Freiser. Therefore, we accept the weighted average of the measurements from reactions 6 and 10, 3.13 ± 0.04 eV, as our best determination of the $CoOH^+$ bond energy at 0 K and conclude that reactions 7 and 17 exhibit thresholds that are higher than their thermodynamic endothermicities (thus leading to calculated Co^+–OH bond energies that are lower than the other values). This conclusion is consistent with the observation that the associated reactions 8a and 18a also exhibit thresholds, even though both reactions are exothermic.

We note that the Co^+–OH bond energy is considerably larger than $D_0(Co^+–CH_3)$ and $D_0(Co^+–H)$, Table 1, even though OH, CH_3, and H can form only one covalent bond with another species. The enhancement in the metal ion–hydroxide bond energy is due to donation of the two lone pairs of electrons on oxygen into half-occupied 3d orbitals on Co^+, as discussed in more detail elsewhere.[8,9]

(b) $CoCH_3^+$. The measured threshold for reaction 11, 1.84 ± 0.08 eV, coupled with $D_0(CH_3–OD)$ = 3.940 ± 0.005 eV yields a bond energy of $D_0(Co^+–CH_3)$ = 2.10 ± 0.08 eV. This value is in good agreement with the value of 2.10 ± 0.04 eV, obtained from previous studies in our laboratory.[35]

(c) CoD^+ and CoH. The threshold measured for reaction 5, 3.16 ± 0.05 eV, coupled with $D_0(DO–D)$ = 5.212 ± 0.001 eV, Table 1, leads to $D_0(Co^+–D)$ = 2.05 ± 0.05 eV, in good agreement with our previous value, 2.01 ± 0.06 eV.[36] In contrast, the measured thresholds for reactions 9 and 14 cannot be used to derive accurate values for $D(Co^+–D)$ because of the strong competition from other major reaction channels.

The measured threshold for reaction 12, 1.89 ± 0.06 eV, Table 2, can be used to derive the bond energy of neutral cobalt hydride by using eq 25,

$$D_0(Co–H) = D_0(DOCH_2^+–H^-) - E_0 - IE(Co) + EA(H) \quad (25)$$

where $D_0(DOCH_2^+–H^-)$ is assumed to equal $D_0(HOCH_2^+–H^-)$ = 10.89 ± 0.01 eV,[37] IE(Co) is the ionization energy of Co, 7.864 ± 0.001 eV, and EA(H) is the electron affinity of H, 0.754 eV.[2]

(33) Carlin, T. J.; Sallans, L.; Cassady, C. J.; Jacobson, D. B.; Freiser, B. S. *J. Am. Chem. Soc.* **1983**, *105*, 6320. Cassady, C. J.; Freiser, B. S. *J. Am. Chem. Soc.* **1985**, *107*, 1566.

(34) Clemmer, D. E.; Sunderlin, L. S.; Armentrout, P. B. *J. Phys. Chem.* **1990**, *94*, 3008. Clemmer, D. E.; Armentrout, P. B. *J. Phys. Chem.* **1991**, *95*, 3084.

(35) Fisher, E. R.; Sunderlin, L. S.; Armentrout, P. B. *J. Phys. Chem.* **1989**, *93*, 7353. The value cited here has been reevaluated to 0 K, as discussed in ref 9.

(36) Elkind, J. L.; Armentrout, P. B. *J. Phys. Chem.* **1986**, *90*, 6576.

(37) Calculated from information given in Traeger, J. C.; Holmes, J. L. *J. Phys. Chem.* **1993**, *97*, 3453.

This gives a bond energy of $D_0(Co–H) = 1.89 \pm 0.06$ eV, in good agreement with previous results from our laboratory, 1.86 ± 0.05 eV.[38]

(d) $CoOCH_3^+$. The estimated threshold for reaction 15, 1.5 ± 0.3 eV, leads to $D_0(Co^+–OCH_3) = 3.0 \pm 0.3$ eV, consistent with a lower limit of 1.8 eV that can be derived from work of Freiser and co-workers.[33] Our value seems reasonable when compared with $D_0(Co^+–OH) = 3.13 \pm 0.04$ eV, Table 1. Also, this threshold indicates that $D_0(CoO^+–CH_3) = 3.6 \pm 0.3$ eV, comparable to the C–O bond energy in methanol, $D_0(H_3C–OH) = 3.93$ eV. In contrast, the measured threshold for reaction 20, 2.15 ± 0.05 eV, leads to much smaller values, $D_0(Co^+–OCH_3) = 1.72 \pm 0.08$ eV and $D_0(OCo^+–CH_3) = 2.33 \pm 0.05$ eV. The latter bond energy is comparable to $D_0(Co^+–CH_3) = 2.10 \pm 0.04$ eV, suggesting that reaction 20 actually forms a different isomer, $OCo^+–CH_3$, rather than the cobalt–methoxy ion. Because it is possible that the relatively minor reactions 15 and 20 are suppressed by the other major reaction channels, these bond energies are most conservatively viewed as lower limits.

(e) $Co^+(CH_3OH)$. The bond energy of $Co^+–CH_3OD$ is directly measured from the threshold of reaction 22, Table 2. The effects of deuterium substitution on this bond energy should be small, and therefore this threshold, 1.53 ± 0.08 eV, should also be a measurement of $D_0(Co^+–CH_3OH)$. It is interesting to note that this bond energy is slightly smaller than $D_0(Co^+–H_2O) = 1.67 \pm 0.06$ eV,[39] although the values are at the edge of the combined experimental errors. It is not clear whether this small difference is statistically significant, but it might be rationalized because the dipole moment of methanol is smaller than that of water.

Discussion

Reaction Mechanisms and Potential Energy Surfaces. (a) $Co^+ + D_2O$ and $CoO^+ + D_2$. There are two reasonable mechanisms for the interaction of Co^+ with D_2O: Co^+ insertion into a D–OD bond to form a D–Co^+–OD intermediate, **I**, or direct abstraction of the D atom or the OD group by Co^+. Oxidative addition of a covalent bond to first-row transition metal ion centers is believed to be most facile when the metal has an empty 4s orbital to accept the pair of electrons in the covalent bond, and when it has a pair of 3d electrons of proper symmetry to donate into the antibonding orbital for the bond.[40] The $^3F(3d^8)$ ground state[41] of Co^+ has a suitable electron configuration for this oxidative addition reaction. Moreover, if the Co–D and Co–OD bonds in the insertion intermediate are covalent, then there will be six nonbonding electrons in four orbitals closely spaced in energy such that this species should have a triplet spin ground state. Thus, formation of **I** from the ground state $Co^+(^3F) + D_2O(^1A_1)$ reactants should conserve spin.

Clearly, intermediate **I** can decompose to form $CoD^+ + OD$, reaction 5, and $CoOD^+ + D$, reaction 6, by simple bond fissions. Both reactions conserve spin as both neutral products have doublet spin and both ionic products have quartet spin.[42] The strong competition observed between these two reactions is consistent with a common intermediate, which is depleted by both reaction channels. A direct abstraction mechanism cannot easily account for this competition, although direct pathways could contribute to the observed reactions, especially at higher kinetic energies.

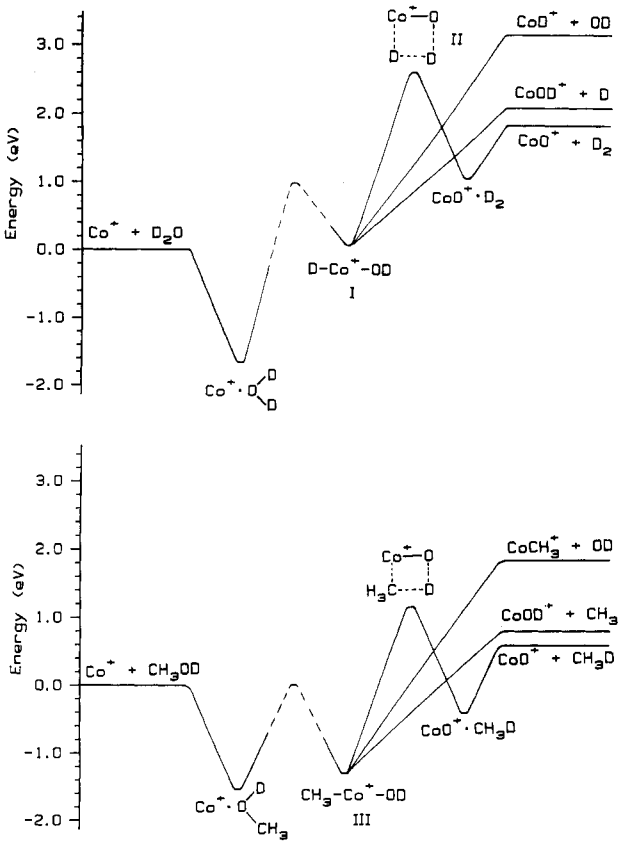

Figure 6. Qualitative potential energy surface for the reaction of Co^+ with ROD, R = D (top, a) and CH_3 (bottom, b), through a R–OD bond insertion mechanism. Electronic details for the $CoO^+ + RD$ channel are not indicated. Dashed lines indicate that no experimental information is available to allow a quantitative estimate of the energy.

Chart 1

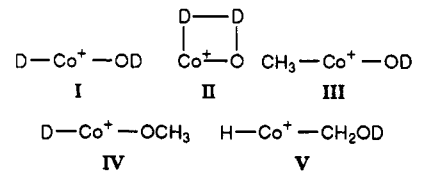

Figure 6a shows a qualitative potential energy surface for the $Co^+ + D_2O$ reaction. The initial interaction is attractive because of the long-range ion–dipole potential. Thus, there is a well corresponding to the $Co^+ \cdot OD_2$ complex, which has a $^3B_2$ ground state according to theoretical calculations.[43] The energy of this complex is taken as the $Co^+–OH_2$ bond energy, 1.67 ± 0.06 eV, Table 1.[28,39,44] The energy of intermediate **I** is estimated to be 0.07 ± 0.07 eV, based on the bond additivity assumption that $D_0(DOCo^+–D) \approx D_0(Co^+–D)$, Table 1. (Although this assumption may not be quantitatively accurate, it is the only reasonable means of estimating the energy of **I**.) The transition state between the $Co^+ \cdot OD_2$ complex and **I** is likely to correspond to a barrier, as discussed further below, but the height of this barrier cannot be quantitatively assessed from our experiments other than to note that it cannot be higher than the energy of the $CoOD^+ +$ D products, because the threshold measured for reaction 6 is the

(38) Fisher, E. R.; Armentrout, P. B. *J. Phys. Chem.* **1990**, *94*, 1674. The value cited here has been reevaluated to 0 K, as discussed in ref 9.

(39) Dalleska, N. F.; Honma, K.; Sunderlin, L. S.; Armentrout, P. B. *J. Am. Chem. Soc.* **1994**, *116*, 3519.

(40) For recent reviews, see Armentrout, P. B. *Science* **1991**, *251*, 175. Armentrout, P. B. *Annu. Rev. Phys. Chem.* **1990**, *41*, 313. *Selective Hydrocarbon Activation: Principles and Progress*, Davies, J. A., Watson, P. L., Greenberg, A., Liebman, J. F., Eds.; VCH: New York, 1990; p 467.

(41) Sugar, J.; Corliss, C. *J. Phys. Chem. Ref. Data* **1985**, *14*, 731.

(42) CoH^+ has a ground state of $^4\Phi$ (Pettersson, L. G. M.; Bauschlicher, C. W.; Langhoff, S. R. *J. Chem. Phys.* **1987**, *87*, 481). $CoCH_3^+$ has a ^4E ground state (Bauschlicher, C. W.; Langhoff, S. R.; Partridge, H.; Barnes, L. A. *J. Chem. Phys.* **1989**, *91*, 2399). If the Co^+–OD bond has covalent character, which seems certain, then it also should have a quartet spin ground state. CH_3 has a ground state of $^2A_2''$ (Jacox, M. E. *J. Phys. Chem. Ref. Data*, **1984**, *13*, 945). OD and D_2 have $^2\Pi$ and $^1\Sigma_g^+$ ground states, respectively (Huber, K. P.; Herzberg, G. *Molecular Spectra and Molecular Structure, IV. Constants of Diatomic Molecules*, Van Nostrand Reinhold: New York, 1979).

(43) Rosi, M.; Bauschlicher, C. W., Jr. *J. Chem. Phys.* **1990**, *92*, 1876.

(44) Marinelli, P. J.; Squires, R. R. *J. Am. Chem. Soc.* **1989**, *111*, 4101.

thermodynamic one. No barriers in excess of the endothermicity to formation of $CoOD^+ + D$ or $CoD^+ + OD$ are found experimentally, consistent with simple bond fission reactions from I. The former product channel is favored thermodynamically, but the latter channel is favored kinetically due to angular momentum considerations, as noted above.

Although formation of $CoO^+ + D_2$ is the most favorable channel thermodynamically, it is not observed for two reasons. First, there is a barrier to this channel in excess of the endothermicity, as exhibited for the reverse reaction 8a, exothermic by 1.86 ± 0.05 eV. Second, this barrier corresponds to a tight transition state and hence this channel is kinetically hindered, as suggested by the failure to observe $CoO^+ + D_2$ products even when sufficient energy to overcome the barrier is supplied to $Co^+ + D_2O$ reactants. We attribute this tight transition state to the four-centered transition state II, Figure 6a, in which the D_2 adds across the CoO^+ bond. This is based on our previous detailed discussion of the reactions of D_2 with ScO^+, TiO^+, and VO^+,[7] in which three possible mechanisms were considered: addition at the metal end of MO^+, addition at the O end, or addition across the MO^+ bond. Molecular orbital considerations suggested that the latter should be the most facile pathway.[7] For similar reasons, we discount the possibility that a direct abstraction reaction of $CoO^+ + D_2$ to form $CoOD^+ + D$ is a *low energy* (barrierless) pathway because this mechanism would involve the interaction of D_2 with the oxygen end of CoO^+ (where there are no empty or half-filled orbitals).

This potential energy surface also allows our observations regarding the reverse reaction of $CoO^+ + D_2$ to be easily understood. The initial long-range ion-induced dipole interaction between CoO^+ and D_2 may lead to the formation of $CoO^+ \cdot D_2$, and we estimate the strength of this interaction as comparable to that measured by Kemper et al. for $Co^+ \cdot H_2$, 0.79 ± 0.04 eV.[45] No further reaction can take place until the barrier corresponding to II is overcome. Thus, formation of both $Co^+ + D_2O$ and $CoOD^+ + D$ is observed to have a common threshold, because these processes have thermodynamic thresholds below the barrier height. We take the barrier height to be 0.75 ± 0.04 eV above the $CoO^+ + D_2$ asymptotic energy, the threshold measured for reaction 7 and consistent with but more precise than that measured for reaction 8a.

Initially, we thought that the observation that $CoOD^+ + D$ formation is more favorable than $Co^+ + D_2O$ formation might suggest that there is a sizable barrier between $Co^+ \cdot OD_2$ and intermediate I, otherwise the transiently formed I should efficiently eliminate water because this channel is thermodynamically much more favorable. The presence of a barrier would mean that this channel is kinetically hindered and therefore does not compete effectively with the simple bond fission leading to $CoOD^+ + D$. Phase space theory (PST) calculations for this system, see below, find that this nonintuitive branching ratio is partially explained by statistical considerations, namely that the density of ro-vibrational states for $CoOD^+$ increases more rapidly than that for D_2O. Including a barrier between $Co^+ \cdot OD_2$ and intermediate I seems intuitively reasonable and can help the PST calculations reproduce the experimental behavior, but the calculations indicate that such a barrier need not be large in order to explain the data.

In contrast to the reaction of $Co^+ + D_2O$, formation of $CoD^+ + OD$ from $CoO^+ + D_2$ is not dominant at high energies, because angular momentum considerations do not play as significant a role, as noted above. This is a combination of the change in reduced mass of the reactants and the differing energetics. As in the $Co^+ + D_2O$ system, direct abstraction reactions may also contribute to the reactivity observed for $CoO^+ + D_2$, but such a mechanism cannot easily explain the competition between the formation of $CoOD^+ + D$ and $Co^+ + D_2O$, nor the observation of $CoD^+ + OD$.

(45) Kemper, P. R.; Bushnell, J.; van Koppen, P.; Bowers, M. T. *J. Phys. Chem.* **1993**, *97*, 1810.

(b) $Co^+ + CH_3OD$ and $CoO^+ + CH_4$. On the basis of the similarities in the reaction cross sections, we propose that the reaction mechanism and potential energy surfaces for the activation of the C–O bond of methanol by Co^+ and for the reaction of CoO^+ with CH_4 are quite similar to those for the $Co^+ + D_2O$ and $CoO^+ + D_2$ reaction systems. This is shown in Figure 6b, where the energies of the various intermediates are estimated as above. The primary difference between the two systems is the energetics of the $Co^+ + ROD$ species and the $Co^+ \cdot ROD$ adduct (where R = D or CH_3) relative to all other channels and intermediates.

Differences in the product distributions between the forward and reverse reactions are now easily understood. For the $CoO^+ + CH_4$ system, addition of a C–H bond across the CoO^+ bond can lead to two intermediates, CH_3–Co^+–OH (III) and H–Co^+–OCH_3 (IV). Because $CoOH^+$ is the major ionic product observed in this reaction, Figure 4, the formation of the former intermediate is clearly favored. This can be rationalized on the basis that an O–H bond is stronger than a C–O bond, but the Co^+–H and Co^+–CH_3 bond strengths are similar, Table 1. Indeed, our analysis of the $CoOCH_3^+$ product formed in reaction 20 can be interpreted to indicate that intermediate IV may not be formed at all. As noted above, the threshold measured for reaction 20 is more consistent with formation of OCo^+–CH_3, which can be formed directly from III by H atom loss, than it is with formation of a cobalt methoxy ion, Co^+–OCH_3, which could be formed easily from IV. The CoH^+ product observed, Figure 4, may suggest that intermediate IV is formed, but its measured threshold is more consistent with $CH_2O + H$ neutral products than with CH_3O as would be expected for a simple bond fission from IV. The mechanism for $CoH^+ + CH_2O + H$ formation from III is necessarily complex, but a rearrangement of the OCo^+–CH_3 product to the more stable Co^+–OCH_3 isomer is a plausible first step.

In addition to activation of the H_3C–OD bond, the Co^+ ion can also activate the CH_3O–D or H–CH_2OD bond of the CH_3OD molecule to form the D–Co^+–OCH_3 (IV) or H–Co^+–CH_2OD (V) intermediates. V cannot be formed directly from the $CoO^+ + CH_4$ reactants and hence products resulting from this intermediate, $CoH^+ + CH_2OD$ and $CH_2OD^+ + CoH$, are absent in Figure 4. The presence of IV in the reaction of $Co^+ + CH_3OD$ is suggested by the observation of $CoD^+ + OCH_3$ (where the measured threshold, 2.80 ± 0.12 eV, is closer to the thermodynamic threshold for OCH_3 as the neutral product, 2.52 ± 0.07 eV, than that for CH_2OH as neutral product, 2.15 ± 0.06 eV) and $CoOCH_3^+ + D$ (where the threshold is consistent with the cobalt methoxy ion isomer, as discussed above).

Finally, the reaction of Co^+ with CH_3OD forms $CoCH_2^+ + HOD$, which can be formed by eliminating HOD from the CH_3–Co^+–OD or H–Co^+–CH_2OD intermediates. Presumably, this must proceed through a tight transition state, thereby explaining why the reaction is inefficient and has a measured threshold exceeding its thermodynamic value. We assign the measured threshold of 0.90 ± 0.08 eV to the height of this barrier relative to the $Co^+ + CH_3OD$ reactants (0.68 ± 0.10 eV relative to products). We note that this barrier is comparable to the barrier leading to $CoO^+ + CH_3D$, 1.16 ± 0.06 eV relative to reactants (0.75 ± 0.04 eV relative to products). This latter process is not observed, presumably because of competition with formation of $CoOD^+ + CH_3$, which has a threshold *lower* than the barrier height. The simplest explanation for why the $CoCH_2+ + HDO$ products are observed is that this reaction proceeds by intermediate V, where the competing bond fission processes leading to $CoH^+ + CH_2OD$ and $CH_2OD^+ + CoH$ do not begin until energies *higher* than the barrier. Indeed, the $CoCH_2+$ cross section does level off near the thresholds for these channels, Figure 3.

Comparison of $D_2 + CoO^+$ Reactivity with That of $D_2 + Co^+$, ScO^+, TiO^+, and VO^+. In our study of the reactions of ScO^+,

TiO^+, and VO^+ with D_2,[7] insight into the details of the reactivity of MO^+ was gained by comparing these systems to the results for reaction of the bare metal ions with D_2, reaction 26.

$$M^+ + D_2 \rightarrow MD^+ + D \qquad (26)$$

The analogous process to reaction 26 for the metal oxides is formation of $MOD^+ + D$. In the present system, the maximum magnitude of $\sigma(CoOD^+)$ formed from the reaction of $CoO^+ + D_2$ is $\sim$2.0 Å^2, Figure 2, similar to the $\sim$1.8 Å^2 magnitude measured for the reaction of $Co^+(^3F)$.[36] This similarity in magnitudes is found despite the fact that reaction 26 is endothermic by 2.55 ± 0.06 eV for Co^+ while reaction 7 is endothermic by only 0.22 ± 0.06 eV (based on the thermochemistry measured here). The barrier shifts the observed threshold for reaction 7 to 0.75 ± 0.04 eV, but thermodynamically, reaction 7 is still much more favorable than reaction 26. This suggests that there is some additional kinetic constraint in the efficiency of reaction 7.

It is also interesting to compare the reactivity of $CoO^+ + D_2$ with that of ScO^+, TiO^+, and $VO^+ + D_2$.[7] In the latter three systems, formation of $MOD^+ + D$ is endothermic by 1.6–2.2 eV, with no barriers in excess of the reaction endothermicity. Note that these endothermicities are sufficiently large that they would exceed the height of a barrier similar to that measured here for the M = Co system. The same is true for the endothermicities for production of $M^+ + D_2O$ in these three early metal systems. Thus, the failure to observe a barrier in these three systems is still consistent with the observation of a barrier in the cobalt system. The magnitudes of the MOD^+ cross sections are essentially constant with a maximum value of about 1.0 Å^2. In the $CoO^+ + D_2$ system, the magnitude of $\sigma(CoOD^+)$ is only twice as large, Figure 2, even though the reaction exhibits a threshold of only 0.75 eV. [A difference in reactivity of two to four is obtained if values of σ_0 are compared, which is reasonable because all four cross sections have similar energy dependencies, i.e., n in eq 4 is about 2.] This comparison again suggests that there is a restriction in the CoO^+ reaction system not present for the early transition metal oxide ion systems.

Electronic States of CoO^+ and the Activation Barrier. The conversions of CH_4 to CH_3OH and of D_2 to D_2O by CoO^+ are exothermic reactions, and we previously[7] anticipated that these reactions might be efficient because of this. Instead, the present study shows that they are inefficient due to the restrictions of activation barriers and other kinetic constraints. To understand the origins of these restrictions, we need to examine the electronic states of CoO^+ and the molecular orbital interactions of these states with methane and deuterium.

Unfortunately, nothing is known experimentally about the electronic states of CoO^+, although Carter and Goddard[46] predicted that CoO^+ may have a $^3\Sigma^-$ ground electronic state based on their calculations for VO^+ and RuO^+. Here, we evaluate the likely low-energy states of CoO^+ by drawing analogies with FeO^+, noting that the 4s orbital is lower in energy for Fe than for Co (because the ground state of Fe^+ is $4s3d^6$, while that for Co^+ is $3d^8$). The ground state of FeO is known to be $^5\Delta$,[47] with a valence electron configuration of $8\sigma^2 3\pi^4 9\sigma^1 1\delta^3 4\pi^2$. Ionization from the three higher molecular orbitals leads to states for FeO^+ of $^4\Phi(8\sigma^2 3\pi^4 9\sigma^1 1\delta^3 4\pi^1)$, $^6\Sigma^+(8\sigma^2 3\pi^4 9\sigma^1 1\delta^2 4\pi^2)$, and $^4\Delta(8\sigma^2 3\pi^4 9\sigma^0 1\delta^3 4\pi^2)$. Recent calculations of Fiedler et al.[48] indicate that the $^6\Sigma^+$ state is the ground state of FeO^+ with the $^4\Phi$ higher in energy by 0.8 eV. The $^4\Delta$ state is about 1 eV higher than the ground state, as calculated at a lower level of theory.[49] For CoO, the ground state is $^4\Delta(8\sigma^2 3\pi^4 9\sigma^2 1\delta^3 4\pi^2)$,[47] but $^4\Sigma^-(8\sigma^2 3\pi^4 9\sigma^1 1\delta^4 4\pi^2)$ is probably low-lying.[50] Ionization from the three higher molecular orbitals of both states leads to states for CoO^+ of $^3\Phi(8\sigma^2 3\pi^4 9\sigma^2 1\delta^3 4\pi^1)$, $^5\Sigma^+(8\sigma^2 3\pi^4 9\sigma^2 1\delta^2 4\pi^2)$, $^5\Delta(8\sigma^2 3\pi^4 9\sigma^1 1\delta^3 4\pi^2)$, $^3\Pi(8\sigma^2 3\pi^4 9\sigma^1 1\delta^4 4\pi^1)$, and $^3\Sigma^-(8\sigma^2 3\pi^4 9\sigma^0 1\delta^4 4\pi^2)$. Based on the comparison with FeO^+, it seems likely that either $^5\Sigma^+$ or $^5\Delta$ is the ground state of CoO^+ with $^3\Phi$ and $^3\Pi$ being low-lying excited states and the $^3\Sigma^-$ state lying somewhat higher in energy. After this paper was submitted for publication, we received results of ab initio calculations on CoO^+ performed by Fiedler et al.[51] They obtain a $^5\Delta$ ground state and excited states of $^3\Sigma^-$ at 1.0 eV, $^3\Pi$ at 1.2 eV, and $^3\Delta$ at 1.4 eV, confirming the qualitative considerations given above.

In our previous paper,[7] analysis of the molecular orbital (mo) interactions between MO^+ and H_2 or CH_4 suggested that the oxidation reactions should be efficient when the metal oxide has an empty mo that can accept electron density from the bond to be broken and an occupied mo having the correct symmetry to donate electron density into the antibonding mo of the bond to be broken. Likely acceptor and donor mos were identified as 9σ and either 3π or 4π, respectively. ScO^+, TiO^+, and VO^+ all have ground-state electron configurations that meet these criteria, thereby explaining why they react efficiently with D_2 despite high reaction endothermicities.

In our previous analysis of the likely reactivity of CoO^+,[7] we assumed that the ground state of CoO^+ was $^3\Sigma^-$, because this state correlates to ground state $Co^+(^3F,3d^8)$, in contrast to the conclusions reached above based on the calculations of Fiedler et al.[48,51] The $^3\Sigma^-$ state has an empty 9σ and occupied 3π and 4π molecular orbitals. Thus reaction 3 was predicted to be efficient because it conserves spin and $CoO^+(^3\Sigma^-)$ has a favorable electron configuration for reaction. If the ground state of CoO^+ is $^5\Delta$ or $^5\Sigma^+$, however, inefficient reaction with D_2 and CH_4 is easily rationalized. These CoO^+ states have occupied 9σ orbitals, leading to more repulsive interactions with D_2 and CH_4. Likewise, the high-lying $^3\Phi$ and $^3\Pi$ states of CoO^+ may have repulsive interactions with these molecules because they have an occupied 9σ orbital as well. These considerations also explain the relative inefficiency of reaction 7 compared to that of reaction 26, as noted above. CoO^+ has an occupied 9σ mo while Co^+ has an empty 4s acceptor orbital, and the additional kinetic constraint to reaction 7 is that this reaction no longer conserves spin while reaction 26 does.

If this mo picture is qualitatively correct, we speculate that the potential energy surfaces for interaction of CH_4 (and D_2 by analogy) with CoO^+ in these various states may be as shown in Figure 7. The excited $CoO^+(^3\Sigma^-)$ state is presumed to bind CH_4 (or D_2) more strongly and with a shorter bond distance than the other states where the 9σ mo is occupied. This surface then diabatically leads to formation of the ground-state R–Co^+–OH intermediate, and from there to the other products observed. Crossings between the quintet and triplet surfaces can interact by spin–orbit coupling. The barrier height measured in this study can be associated with the barrier along either the low-spin surface, Figure 7a, or the high-spin surface, Figure 7b. In the former case, the observed reactivity occurs by transferring from the high-spin to the low-spin surface, thereby explaining the inefficient reactivity as due to the spin-forbidden nature of the reaction. In the latter case, the observed reactivity occurs in a spin-allowed fashion along the high-spin surface, thereby explaining the inefficient reactivity as due to reaction along an unfavorable excited state surface. Clearly, these qualitative potential energy surfaces can be improved as more advanced information regarding the states of CoO^+ becomes available.

The surfaces shown in Figure 7b are consistent with those

(46) Carter, E. A.; Goddard, W. A., III *J. Phys. Chem.* **1988**, 92, 2109.
(47) Merer, A. J. *Annu. Rev. Phys. Chem.* **1989**, *40*, 407.
(48) Fiedler, A.; Hrušák, J.; Koch, W.; Schwarz, H. *Chem. Phys. Lett.* **1993**, *211*, 242.
(49) Krauss, M.; Stevens, W. J. *J. Chem. Phys.* **1985**, *82*, 5584.
(50) Green, D. W.; Reedy, G. T.; Kay, J. G. *J. Mol. Spectrosc.* **1979**, *78*, 257.
(51) Fiedler, A.; Schröder, D.; Shaik, S.; Schwarz, H. *J. Am. Chem. Soc.*, submitted for publication; personal communication.

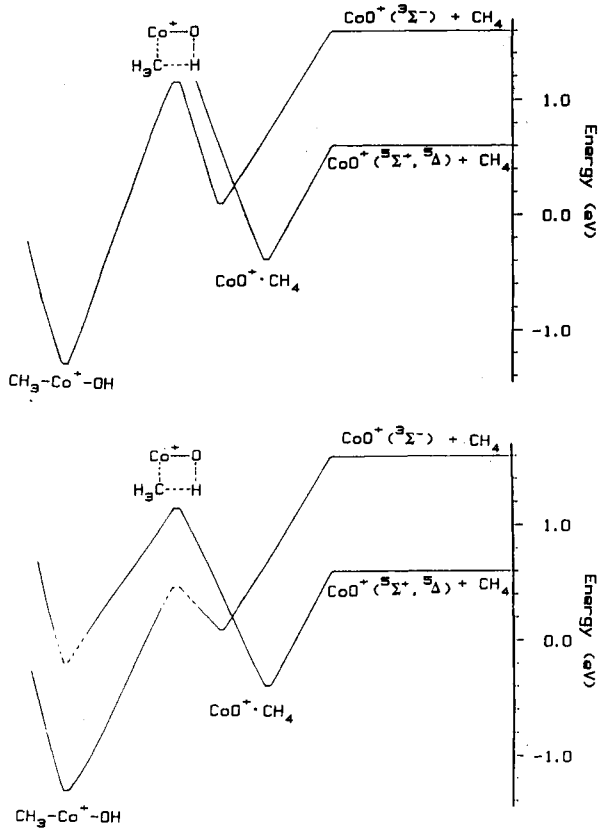

Figure 7. Two possible qualitative potential energy surfaces for the reaction of CH_4 with the triplet and quintet states of CoO^+. The energies of these states are estimated, see text for details. Dashed lines indicate that no experimental information is available to allow a quantitative estimate of the energy.

derived for the reaction of FeO^+ with D_2,[52] where the electronic details are believed to be very similar. The only difference in the reaction behavior between the two reaction systems is that an inefficient but barrierless pathway is also observed for the reaction analogous to process 8a in the iron system. This observation is discussed in more detail in this other paper, but we speculate that this reactivity corresponds to crossing from the surface of the high-spin reactant to the low-spin surface leading to intermediate I. Because this channel is observed to have no energy barrier, this means that the surface crossing *and* the barrier corresponding to II on the low-spin surface are below the energy of the $FeO^+ + D_2$ ground-state reactant asymptote. Our observations in the cobalt system can be rationalized by imagining that either the surface crossing or this barrier is *above* the $CoO^+ + D_2$ ground-state reactant asymptote, thereby making this process even more inefficient.

In this speculative model, the energy of the barrier is influenced by three factors: the energy of the insertion intermediate I relative to the ground $CoO^+ + RH$ reactants, the excitation energy of the $CoO^+(^3\Sigma^-)$ state, and the depth of the potential well for $CoO^+ \cdot RH$. These features may help explain the relative heights of the activation barriers in the methane, 0.56 ± 0.08 eV, and D_2, 0.75 ± 0.04 eV, systems. This result is the opposite of that expected on the basis of theoretical calculations, which find that the energies of transition states associated with C–H bond activation by neutral metal atoms are on the order of 0.4 eV higher than those associated with H–H bond activation.[53,54] This is largely because of the directionality of the CH_3 bonding orbital compared to the spherical hydrogen atom. For the present system, the bond strength of CH_3–H is 0.08 eV weaker than that of D–D and the Co^+–CH_3 bond is 0.09 eV stronger than the Co^+–D bond, Table 1. The depths of the potential wells of $CoO^+ \cdot RH$ complexes are estimated as equivalent to $D_0(Co^+–CH_4)$ = 0.99 eV for RH = CH_4 and $D_0(Co^+–H_2)$ = 0.79 eV for RH = D_2.[45,55] Apparently, these thermodynamic factors allow the barrier for activation of methane to move below that for activation of deuterium, such that activation of C–H bonds is facilitated by interaction with metal oxide ions compared to that with bare metals.

Consideration of Kinetic and Competitive Shifts. Phase Space Modeling. Although the picture of these reaction sytems developed above is self-consistent, it is important to consider the possibility that the thresholds for reactions 7 and 8a might be affected by kinetic shifts, i.e., that these reactions take a longer time than that available in our experimental apparatus and hence the first observation of a reaction is delayed until an energy where the kinetics are sufficiently fast that we observe them. We first note that a kinetic shift, if it exists, can only be influencing our measurement of the height of the barrier, not whether there is a barrier along the potential energy surfaces for these reactions. This is based on our observation of common thresholds for reactions 7 and 8a and reactions 17 and 18a, pairs of reactions that have very different energetics and almost certainly have very different kinetics.

In considering the kinetic question further, it should be remembered that kinetic shifts are usually discussed in terms of unimolecular reactions where kinetic shifts occur because an energized ion does not dissociate on the experimental time scale. Thus, the parent ion is observed rather than the product ions. In the bimolecular reactions studied here, kinetic shifts would occur when the energized molecule formed from the reactants (i.e. $CoO^+ \cdot D_2$ or $CoO^+ \cdot CH_4$, the adducts of the reactants) is observed rather than the product ions. In our apparatus, the flight time of the ions from the collision chamber to the detector quadrupole is about 10^{-4} s. It seems highly unlikely that the $CoO^+ \cdot D_2$ or $CoO^+ \cdot CH_4$ species have lifetimes exceeding this, and indeed no adduct species were observed in our studies within a limit of better than 10^{-2} Å^2. If kinetic shifts were to explain the discrepancy between our observations and those of Schröder et al.,[11] who observed reaction 8a with the rate constant of 1.2×10^{-12} cm^3 s^{-1}, then we should have seen the $CoO^+ \cdot D_2$ adduct with a cross section of 3×10^{-2} Å^2.

Another possible way that the thresholds measured here could be shifted from the true barrier height is if there is severe competition between the channels of interest and some other channel. In the $CoO^+ + D_2$ reaction system, these are the $CoOD^+ + D$ and $Co^+ + D_2O$ product channels, where the only possible competitive channel is dissociation of the $CoO^+ \cdot D_2$ adduct to reform the $CoO^+ + D_2$ reactant ions (a process that we cannot observe directly). Under the conditions used in these experiments, we can observe reaction efficiencies as small as 10^{-4}, such that this competition must favor reforming the reactants by a factor larger than 10^4, otherwise we would observe the $CoOD^+ + D$ and $Co^+ + D_2O$ products. Similar considerations hold for the analogous methane system.

To further test whether this type of competition could influence our measurement of the reaction thresholds, we have carried out a phase space theory (PST) calculation for the reaction of CoO^+ with D_2. We have previously detailed our use of PST for this type of calculation,[56] and use codes that are adapted from those of Bowers, Chesnavich, and others.[57] In a PST calculation, reactions are assumed to proceed through a strongly coupled

(52) Clemmer, D. E.; Chen, Y.-M.; Khan, F. A.; Armentrout, P. B. *J. Phys. Chem.*, accepted for publication.
(53) Low, J. J.; Goddard, W. A. *J. Am. Chem. Soc.* **1984**, *106*, 8321.
(54) Blomberg, M. R. A.; Siegbahn, P. E. M.; Nagashima, U.; Wennerberg, J. *J. Am. Chem. Soc.* **1991**, *113*, 424.
(55) Haynes, C. L.; Armentrout, P. B., work in progress.
(56) Weber, M. E.; Dalleska, N. F.; Tjelta, B. L.; Fisher, E. R.; Armentrout, P. B. *J. Chem. Phys.* **1993**, *98*, 7855.
(57) Programs are now available from the Quantum Chemistry Program Exchange, Indiana University, program No. 557. Contributors to the original and revised programs include Bowers, M. T.; Chesnavich, W. J.; Jarrold, M. F.; Bass, L.; Grice, M. E.; Song, K.; Webb, D. A.

Table 3. Molecular Constants (in cm^{-1}) Used in Phase Space Calculations

species	ω_e ($\omega_e X_e$)	*B*
CoO^+	850 (6)[a]	0.5[b]
OD[c]	2720 (44.1)	10.02
D_2[c]	3116 (61.8)	30.44
D_2O[d]	2784 (56.2), 1206 (13.8), 2889 (50.4)	8.18[e]
$CoOD^+$[f]	2400 (42), 700 (6), 300 (4)	1.1, 1.3[e]
CoD^+[g]	1350 (30)	3.7
T.S.[h]	530, 700, 740, 990, 1140	0.62[e]

[a] Estimated from CoO, footnote *c*. [b] Estimated from other first-row transition-metal oxides, footnote *c*. [c] Huber, K. P.; Herzberg, G. *Molecular Spectra and Molecular Structure IV. Constants of Diatomic Molecules*; Van Nostrand Reinhold: New York, 1979. [d] Benedict, W. S.; Gailar, N.; Plyler, E. K. *J. Chem. Phys.* **1956**, *24*, 1139. [e] Treated as a spherical top. [f] Vibrational frequencies are estimated from those of CoO^+ and OD. A rotational constant of 1.3 cm^{-1} was estimated by using structural information for a high-spin H–Fe^+–OH intermediate (except where H is eliminated) calculated in ref 51. A value of 1.1 cm^{-1} is found to match the experimental data better, see text. [g] Vibrational constant is estimated by using a Morse potential to scale the frequency of CoH^+ from: Pettersson, L. G. M.; Bauschlicher, C. W., Jr.; Langhoff, S. R. *J. Chem. Phys.* **1987**, *87*, 481. The rotational constant is calculated from the bond length given there. [h] Transition state in the entrance channel. Vibrational frequencies are estimated from values for the corresponding $CoOCH_2^+$ species as calculated in ref 51. The rotational constant is estimated from the structural information of the analogous $FeOH_2^+$ species as calculated in ref 51.

Table 4. Parameters Used in Phase Space Calculations

reaction channel	reduced mass (amu)	polarizability of neutral ($Å^3$)	symmetry no.[a]	surfaces[b]
$CoO^+(^5\Delta) + D_2(^1\Sigma_g)$	3.82	0.775[c]	2	10(5)
$CoOD^+(^4A) + D(^2S)$	1.96	0.667[d]	1	8(5)
$CoD^+(^4\Phi) + OD(^2\Pi)$	13.90	1.1[e]	1	32(10)
$Co^+(^5F) + D_2O(^1A_1)$	14.94	1.45[f]	2	35(5)

[a] Product of the symmetry numbers for the ionic and neutral species. [b] Electronic degeneracy (assumed number of reactive surfaces). [c] Hirschfelder, J. O.; Curtiss, C. R.; Bird, R. B. *Molecular Theory of Gases and Liquids*; Wiley, New York, 1954; p 947. [d] α(D) assumed to equal α(H) from: Miller, T. M.; Bederson, B. *Adv. At. Mol. Phys.* **1977**, *13*, 1. [e] α(OD) assumed to equal α(OH) which is estimated by using the empirical method of: Miller, K. J.; Savchik, J. A. *J. Am. Chem. Soc.* **1979**, *101*, 7206. [f] $\alpha(D_2O)$ assumed to equal $\alpha(H_2O)$ from: Rothe, E. W.; Bernstein, R. B. *J. Chem. Phys.* **1959**, *31*, 1619.

intermediate, **I** in this reaction system, while total angular momentum and energy are explicitly conserved. Because the common thresholds observed for reactions 7 and 8a suggest that there is an activation barrier due to the four-centered tight transition state in the entrance channel of this reaction system, additional assumptions must be added to PST. As we have outlined elsewhere,[56] we use a theory for translationally driven (TD) reactions as outlined by Chesnavich and Bowers,[58] who adapted a treatment of Marcus.[59]

Table 3 lists the molecular constants for reactants and products used in this calculation, and Table 4 gives other parameters needed for the calculation. Molecular parameters for the four-centered $CoOD_2$+ transition state **II** were taken from calculations by Fiedler et al.[51] for the analogous four-centered transition state for the $FeOH_2$+ system. These calculations include results for both a high-spin and a low-spin transition state and both sets of parameters were tried in our calculations. Endothermicities for reactions 7 and 9 were taken as the literature values given above, and the exothermicity for reaction 8a was taken as 1.34 eV which is the energy for spin-allowed formation of the $Co^+(^5F)$ excited state. The height of the transition-state barrier was allowed to vary to best reproduce the experimental cross sections. Another adjustable parameter in these calculations is the number of reactive

(58) Chesnavich, W. J.; Bowers, M. T. *J. Phys. Chem.* **1979**, *83*, 900.
(59) Marcus, R. A. *J. Chem. Phys.* **1975**, *62*, 1372.

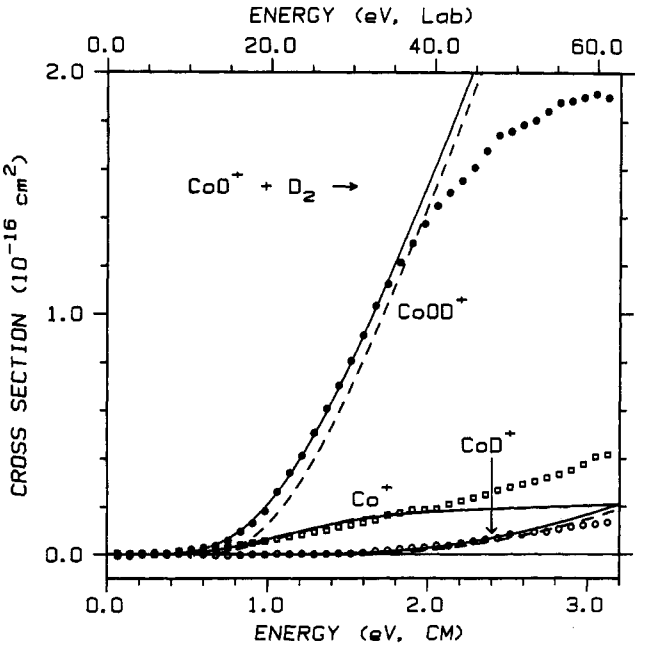

Figure 8. Comparison of experimental results for $CoO^+ + D_2$ with translationally driven phase space theory calculations as a function of kinetic energy in the center-of-mass frame (lower axis) and laboratory frame (upper axis). Symbols show the experimental results, which are the same as in Figure 2. Dashed lines show the theoretical calculations made as described in the text. Solid lines show these calculations convoluted over the experimental energy distributions.

surfaces. For the $CoO^+(^5\Delta) + D_2(^1\Sigma^+_g)$ reactants, which have a total degeneracy of ten, the only reasonable choices are five and ten reactive surfaces with the former value giving better agreement with the experimental data.

The results of this TD-PST calculation are compared with the experimental data in Figure 8. These results were obtained by using parameters for the high-spin transition state. (Parameters for the low-spin species yielded cross sections with magnitudes much lower than experiment.) Without adjusting the parameters for the transition-state **II** or the reactants, theory is easily able to reproduce the absolute magnitude and shape of the total cross section up to about 2 eV. The only adjustable parameters being the number of reactive surfaces 5 and the barrier height, 0.65 ± 0.05 eV. Because this calculation assumes that only translational energy is used to cross the barrier, this barrier height should be compared with that measured above *without* including contributions from the internal energy of the reactants, namely 0.70 ± 0.04 eV. Note that this TD-PST calculation explicitly includes the possibility that the reactants fail to cross the barrier and that the strongly coupled intermediate can also dissociate by recrossing the barrier. The good agreement between this calculation and our data confirms that there are no kinetic or competitive shifts influencing our results. It seems likely that similar conclusions hold for the methane system.

The phase space calculation is also found to reproduce the product branching ratios up to about 2 eV. The results shown in Figure 8 use an estimate for the rotational constant for $CoOD^+$ of 1.1 cm^{-1}, somewhat reduced from our initial estimate of 1.3 cm^{-1}. This change increases the density of states for this channel but does not affect the total cross section for reaction. Alternatively, reasonable agreement could be achieved by invoking an exit channel barrier for elimination of D_2O from intermediate **I**, a possibility discussed above. In this model, the optimum energy for such a barrier was about –0.8 ± 0.2 eV relative to the $CoO^+ + D_2$ reactants. The observation that the TD-PST calculation can reproduce the experimental cross sections of all channels with reasonable fidelity implies that the assumptions of this calculation hold; namely, the reaction proceeds by passing over

a tight transition state at low energies, and then forming a strongly coupled intermediate that dissociates statistically into the three observed channels.

Above 2 eV, the TD-PST calculation deviates from the experimental data. Note that the calculation overestimates the amount of $CoOD^+ + D$ and underestimates the amount of $Co^+ + D_2O$, suggesting that the branching ratio is no longer controlled by statistical factors alone at these elevated kinetic energies. Indeed, the experimental data can be rationalized by noting that as the energy increases, the lifetime of the intermediate becomes shorter, thereby decreasing the time available to randomize energy in all degrees of freedom. In such circumstances, angular momentum conservation becomes increasingly important. Because the reduced mass of the $CoOD^+ + D$ products is less than that of the reactants and much less than that for the $Co^+ + D_2O$ channel, Table 4, the latter channel will be favored by angular momentum considerations while the former will be disfavored.

Summary

Cross sections for the reactions of $Co^+ + D_2O$, $CoO^+ + D_2$, $Co^+ + CH_3OD$, $CoO^+ + CH_4$, and $Co^+(CH_3OD) + Xe$ are reported. The most intriguing observation is that the oxidation of methane and D_2 by CoO^+, both exothermic reactions, does not occur until overcoming activation barriers of 0.56 ± 0.08 and 0.75 ± 0.04 eV, respectively. The behavior of the forward and reverse reactions in both the D_2 and CH_4 systems is consistent with reactions that proceed via the insertion intermediates $R–Co^+–OH$, where $R = CH_3$ or H. Molecular orbital ideas suggest that the activation barrier is likely to correspond to a four-centered transition state associated with addition of RH across the CoO^+ bond. Reasonably detailed potential energy surfaces for both reaction systems are derived from the experimental data. Although the low-lying electronic states of CoO^+ are unknown, they are likely to influence the reaction dynamics and likely possibilities are discussed in some detail. Phase space theory calculations for the $CoO^+ + D_2$ reaction help confirm details of the proposed mechanism and potential energy surfaces.

Analysis of endothermic thresholds for production of CoD^+, CoH, and $CoCH_3^+$ leads to thermochemistry consistent with previous studies in our laboratory and that for $CoOH^+$ and $CoOCH_3^+$ is consistent with work in other laboratories. Thermochemistry for $Co^+(CH_3OH)$ and the $OCoCH_3^+$ isomer is derived here for the first time.

Acknowledgment. This work is supported by the National Science Foundation, Grant CHE-9221241. We thank D. Schröder and H. Schwarz for communicating results before publication and for drawing our attention to the question of a kinetic shift.